Variational Calculation of Specific, Highly Excited Vibrational States in DFCO: Comparison with Experimental Data†

Christophe Iung* and Gauthier Pasin‡

Equipe de Chimie Théorique, Méthodologies et Modélisation, Institut Gerhardt, UMR 5253 CNRS-UMII-ENSCM, CC 014, Université Montpellier II 34095 Montpellier Cedex 05, France

Received: May 4, 2007; In Final Form: July 16, 2007

A stimulated emission pumping spectra of jet-cooled DFCO performed by Crane et al. (*J. Mol. Spectrosc.* **1997**, *183*, 273) has provided a great number of ro-vibrational lines up to 9000 cm^{-1} of excitation energy. By combining a Jacobi−Wilson (JW) approach with a Davidson scheme, we calculate the lines provided by the experiment up to 9000 cm^{-1} using an ab initio global potential energy surface (PES) developed by Kato et al. (*J. Chem. Phys.* **1997**, *107*, 6114). Comparisons between experimental and calculated data provide a critical test of the quality of the PES used. We show that the variational calculated energies can be efficiently corrected by taking into account the error observed for the A' fundamental transitions ν_i ($i = 1, ..., 5$) and the first overtone $2\nu_6$. A detailed analysis of the eigenstates obtained by the calculation allows one to quantify the coupling between the different modes. Such an information is essential to understand and predict the energy flow through a DFCO molecule that is initially excited.

I. Introduction

The intramolecular vibrational-energy redistribution (IVR) is an important energy-transfer mechanism that occurs in all molecules. The IVR process can have a decisive influence on the overall dynamics and reactivity of a molecular system[1,2] for a reaction to occur. The specificities of IVR pathways are extremely diverse depending on the molecular structure of each system. At energies just above the threshold for a given bond dissociation, vibrational energy is required to flow between vibrational modes into the reaction coordinate. It is thus crucial to determine the time scale corresponding to the energy flow through the system. It is also decisive to model this energy flow and to find general rules that govern this phenomenon. The theoretical prediction of the energy flow through an initially excited system requires the knowledge of the potential energy surface (PES) that correctly describes the highly excited states. The calculation of an accurate PES that gives a satisfactory description of highly vibrationally excited system constitutes a real challenge. Comparisons between experimental and simulated spectra provide a critical test of the quality of the PES used to describe the system and to predict its dynamical behavior. From the experimental point of view, different groups have developed with great success very sophisticated experiments to obtain fully resolved spectra of highly excited polyatomic systems such as HFCO,[3] DFCO,[4,5] CF_3H,[6−10] HONO,[11,12] CH_3OH,[8] and C_6H_6,[13−15] for instance. Consequently, it is crucial to develop methods that provide the vibrational spectrum correctly even for highly excited states. The experimental data are more accurate than calculated ones. It is impossible to obtain a vibrational eigenvalue of a polyatomic molecule containing more than four atoms with an error smaller than few cm^{-1} for an excitation energy of about 8000 cm^{-1}. It is possible to calculate with a great accuracy several lines using huge basis sets and very sophisticated variational methods. However, the inaccuracy of the PES generates some errors of few cm^{-1} (ref 16) for such excitation energies. By using some experimental data, it is possible to improve the PES.[17−21] Ab initio calculation of the ro-vibrational spectrum can help the analysis of experimental data for at least two reasons. First, if the eigenstates are provided with the eigenvalues, the eigenstate analysis helps to understand the structure of the experimental spectrum. When intermode couplings are efficient, it is not possible to label an energy level by an unique zero-order state. The analysis of the eigenstates allows to estimate the real role played by the different normal modes in a given eigenstate. Second, a theoretical study can give some time-independent data (the excitation spectrum) but also some time-dependent data (the energy flow through the molecule which has been initially excited). The assignment of the spectrum helps to understand the dynamical behavior of an initially excited system. From the experimental point of view, it is far more difficult to obtain directly some accurate information about the energy flow in a highly excited polyatomic system containing more than four atoms.

At least three different numerical quantum strategies have been explored to calculate the energy of highly excited states that can be located in a dense part of the spectrum. First, one can mention time-dependent methods. Some energy-guided diagonalization was introduced earlier by Neuhauser as the filter diagonalization (FD) scheme.[22,23] In these approaches, a basis of energy-localized wave packets is used to window the spectrum, these wave packets being calculated from the time-dependent propagation of an initial wave function. The MCTDH code developed by the H.-D. Meyer group in Heidelberg[24−26] has been coupled with filtered diagonalization approaches to provide energies of excited ro-vibrational states.[27−30] This approach has given highly excited states in CF_3H,[31] XFCO (X= H or D),[32,33] with a satisfactory accuracy up to 6000 and 18 000 cm^{-1} of excitation energy, respectively. It has been also shown recently that the MCTDH code can provide eigenstates from

† Part of the special issue "Robert E. Wyatt Festschrift".

* Corresponding author. E-mail: iung@univ-montp2.fr.
‡ E-mail: gpasin@univ-montp2.fr.

10.1021/jp0734272 CCC: $37.00
Published on Web 09/20/2007

a propagation by using an improved relaxation method.[27] This new tool has been successfully applied to H_2CS,[34] HONO,[35] and HFCO[36] up to about 8000, 4000, and 6000 cm^{-1} of energy excitation, respectively. Second, one can mention sophisticated time-independent perturbative approaches such as the CVPT method developed by Sibert and co-workers.[37] CVPT has been successfully used to calculate the ro-vibrational spectrum of a large variety of molecules such as H_2CO,[17] CX_4,[18] CH_3OH,[19] and CX_3H (X = Br,F),[20,21] for instance. After an efficient perturbative treatment, a variational calculation is performed in a small basis set characterized by one or few quantum number, $N_j = \sum c_{i,j}\upsilon_i$, which define polyads of states that are significantly coupled (υ_i denotes the occupation number of normal mode i, and $c_{i,j}$ is the polyad characteristic coefficient). CVPT provides an accurate and complete vibrational spectrum, i.e., with excitation energies, labeling of the lines in terms of normal mode quantum number, and line intensities. The advantage of the method stems from the fact that the dimension of the matrix to be diagonalized is smaller than in a variational approach. A comparative study between the use of this CVPT method and a sophisticated variational method has shown that CVPT provides results with an excellent accuracy up to about 7000 cm^{-1} of excitation energy in HFCO.[16] However, this method become less efficient and can be coupled with variational approaches for more excited states.[16] Pouchan and co-workers[38−40] select an adapted active space in which the Hamiltonian is diagonalized to provide fundamental and low-excited combination bands for large system. This approach also combines a variational approach with a perturbative treatment. Third, one can mention variational approaches. A large variety of variational methods have been developed. Wyatt performed pioneer works by developing the recursive residue generated method (RRGM).[41−43] The major goal of this method is the direct computation of the energies and residues, $r_\alpha = |\langle\psi_i|\psi_\alpha\rangle|^2$, without computing the eigenstates where ψ_α is an eigenstate of the system and ψ_i is an initial state chosen by the user. If $\psi_i = \hat{\mu}\Psi_{\text{fund}}$, RRGM provides the spectrum (energies and intensities) of the studied system. This approach coupled with the Lanczos algorithm[44] provides all the energies and residues associated to the eigenvectors whose projection onto the initial state ψ_i is not equal to zero. Wyatt has also contributed actively to the development of a new variational method denoted wave operator sorting algorithm (WASO)[41,45,46] based on the construction of a working active space built by the Wave operator method.[47] The diagonalization of the Hamiltonian expressed in the working active space provides with a very interesting accuracy the eigenenergies and residues. This approach allows to use huge basis sets to describe the system. Consequently, studies of large systems or highly excited ones are possible with this method. WASO has provided some interesting information on the spectra and the dynamics in a large variety of molecules such as CD_3H,[45] CF_3H,[48,49] and C_6H_6[46,50] described by a set of rectilinear normal modes and a primitive basis set containing billion of states. The systematical study of large motions in highly excited systems requires the use of a curvilinear description of the system and a numerical method that provides energies located in a dense part of the spectrum. The straight Lanczos algorithm represents a very efficient and simple method to converge the low-density part of the spectrum. As the convergence becomes very slow for denser part of the spectrum, i.e., at higher energies, spectral transformed Lanczos algorithms[51] can greatly improve it. It consists of using in the Lanczos recursions another operator, $f(\hat{H})$, whose spectrum is strongly dilated around some reference energy E_{ref}. Few Lanczos recursions using $f(\hat{H})$ are required to provide both the eigenvalues and eigenvectors located in the vicinity of E_{ref}. However, computing $f(\hat{H})$ is, in general, very expensive if the density of states is high and if a curvilinear description of the system is used. Wyatt had also proposed some new original strategies to calculate specifically some eigenstates located in a dense part of the spectrum.[52−54] Following these works, Wang and Carrington proposed the PIST method,[55−57] which uses an iterative linear solver in order to compute approximated-transformed Lanczos vectors. Bian and Poirier[58,59] coupled PIST with three different techniques: phase-space optimization discrete variable representation (PSO-DVR),[60] optimal separable basis (OSB),[61] and Wyatt preconditioning.[52]

The outline of this study is as follows. First, the numerical method used to calculate selectively a series of highly excited states in DFCO is presented in Section II. It consists of a Davidson scheme coupled to a Jacobi−Wilson (JW) method, which allows to extract eigenenergies and eigenstates in a dense part of the spectrum. In Section III, a detailed comparison between the experimental data and the numerical spectrum is presented. This analysis constitutes a critical test of the quality of the PES used to describe the system. In Section IV, the intermode couplings are analyzed: their consequences on the structure of the spectrum are discussed. Section V concludes and gives some perspectives.

II. A Davidson Scheme Coupled to a Jacobi−Wilson Parametrization: Application to DFCO

A. The Jacobi−Wilson Parametrization of DFCO. The pioneer study performed by Wyatt and co-workers[41,50] used a rectilinear description of atom motion to study the energy flow through a molecule such as benzene[62−64] or fluoroform[48,49] whose one CH stretch has been excited by two or three quanta of excitation. This rectilinear parametrization was adopted by Wyatt and co-workers in these studies for at least two reasons. First, one of the aims of these studies was to develop a numerical strategy that extracts specific eigenstates and eigenvalues in a system described by a primitive basis set containing billions of states.[41] It was easier to demonstrate the efficiency of this new method (the WASO method,[41,45,46] for instance) using a rectilinear description because the action on a vector of the Hamiltonian expressed with this set of coordinates is faster. However, the use of rectilinear coordinates does not reduce the intermode couplings and does not make easier the extraction of the eigenstates of the system. Consequently, this study demonstrates the robustness and the efficiency of the WASO method to study large systems that are initially excited. Second, expression of the kinetic energy operator (KEO) in terms of curvilinear coordinates can be very intricate. The use of rectilinear coordinates was possible to study IVR in benzene and fluoroform, whose one CH stretch was initially excited by two or three quanta because the energy remains mainly in the CH chromophore (which is constituted by the CH stretch and a XCH bending motion) and is not significantly transferred to the other modes. Consequently, it was only required to provide a 10th order development of the potential[48,49] to describe correctly the large-amplitude motion of the CH chromophore. A more basic description was sufficient for the other normal modes. However, it is not possible to use a rectilinear description to study highly excited states whose energy is very similar to the dissociation energy of the studied system. Consequently, a curvilinear description of atom motion is inescapable to describe highly excited states of DFCO whose dissociation energy is estimated to about 14 000 cm^{-1} above the ground state.

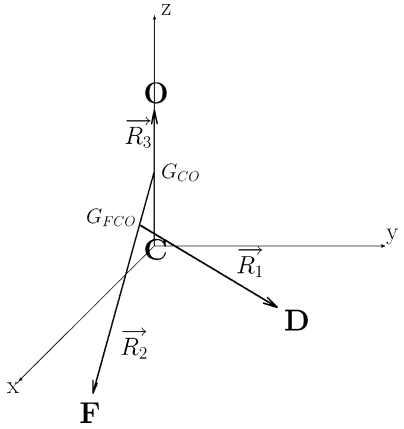

Figure 1. Polyspherical parametrization of DFCO:[69] three Jacobi vectors are used to describe DFCO $\{\vec{R}_1, \frac{D}{\vec{R}_2}, \vec{R}_3\}$. Each vector, $\vec{R}_i$ is parametrized by its spherical coordinates (R_i, ∂_i, θ_i) in a BF frame such that Gz^{BF} is taken parallel to $\vec{R}_3$ and xz^{BF} half-plane ($x > 0$) is parallel to $\vec{R}_2$. Consequently, the six polyspherical coordinates used to parametrize DFCO are: (R_1, R_2, R_3, θ_1, θ_2, φ_1). G_{CO} and G_{FCO} denote the barycenter of (C, O) and (F, C, O) atoms, respectively.

However, the use of developed expression of the KEO in terms of curvilinear coordinates can be very difficult. It is the reason why we adopt, in this study, the Jacobi−Wilson description,[65−68] which combines the simplicity of the exact KEO expressed in terms of polyspherical coordinates[69,70] with the efficiency of the Wilson normal-mode approach.[71] Starting from a description with a set of six polyspherical coordinates denoted $\{q_n, n = 1, ..., 6\}$, corresponding to a Jacobi vector parametrization of the system (see Figure 1), a set of *curvilinear* normal modes, denoted $\{Q_\alpha, \alpha = 1, ..., 6\}$ is introduced to calculate the excitation vibrational spectrum. These *curvilinear* normal mode coordinates are provided by the FG method of Wilson,[71] that is:

$$Q_\alpha = \sum_{n=1}^{6} L_{\alpha n}{}^{-1} q_n \qquad (1)$$

Our corresponding basis functions are eigenfunctions of six uncoupled harmonic oscillators describing the curvilinear normal coordinates. This normal-mode basis can be refined by including the diagonal anharmonicities. Specifically, the basis set B is thus spanned by the product functions $|v_1, v_2, ..., v_6\rangle^0$, where v_i corresponds to the occupation number of the anharmonic oscillator describing the normal-mode Q_i. This basis **B** can be restricted by using several criteria:

(1) First, energy cutoffs can be introduced to limit the dimension of the basis set **B**:

$$\text{If } E^0_{v_1,...,v_6} \le E^{\text{tot}}_{\text{max}} \text{ and } E^{1,3,4,5} \le E^{1,3,4,5}_{\text{max}} \text{ THEN } |v_1,...,v_6\rangle^0 \in \mathbf{B} \quad (2)$$

where $E^{\text{tot}}_{\text{max}}$ represents the maximum allowed total energy, while $E^{1,3,4,5}$ and $E^{1,3,4,5}_{\text{max}}$ are the energy located in modes 1, 3, 4, and 5 in state $|v_1, v_2, ..., v_6\rangle^0$ and the maximum allowed energy in these modes, respectively. This second parameter is introduced because the experimental study[4,5] focuses on states where the energy is mainly located in mode 6 (out-of-plane mode) and mode 2 (CO stretch), which are strongly coupled in DFCO by an efficient Fermi resonance ($\nu_2 \simeq 2\nu_6$). The frequencies of the different vibrational modes in DFCO can be found in Table 1 (column 2). Because of the existence of this Fermi resonance, a study of polyads of coupled states has been performed: a polyad can be characterized by a quantum number N_{26} equal to $v_2 + (v_6/2)$.

TABLE 1: Experimental Fundamental Vibrational Frequencies in DFCO[a]

mode	observed	calculated[b]	$E^{\text{exp}} - E^{\text{calcd}}$	$\Delta\nu_i$
ν_1 (A') (CD stretch)	2261.7	2275.4	−13.7	−14.8
ν_2 (A') (CO stretch)	1796.8	1783.7	13.1	16.9
ν_3 (A') (DCO bend)	967.9	979.8	−11.9	−11.9
ν_4 (A') (CF stretch)	1073.2	1066.2	7.0	7.2
ν_5 (A') (FCO bend)	657.5	653.0	4.5	4.6
$2\nu_6$ (A') (out-of-plane)	1705.8	1715.8	−10.0	−6.5

[a] The first overtone of mode 6 is given because we focus on A' symmetry in the present study. All the quantities are expressed in cm^{-1}. [b] The PES developed by Kato et al.[75] has been used to calculate these frequencies.

(2) Second, one can also impose some constraints ($n_\alpha \le N_\alpha$) on the maximum occupation number of each mode, where n_α is the larger allowed quantum number for mode Q_α. To selectively study one state or a polyad of states, one can define a more specific basis set. This allows us to use a more adapted working basis set. This point is important to converge with a satisfactory accuracy highly excited states.

The use of a global PES to describe the system requires the presence of an underlying pseudospectral scheme of *direct* iterative methods. That is, one defines a 6D grid, **G**, subject to an energy cutoff: $Q_{1a} \times ... \times Q_{6f} \in \mathbf{G}$ if $V_{a,...,f} \le E_G$. By using a grid cutoff larger than the basis cutoff, $E_G = \eta E^{\text{tot}}_{\text{max}}(|v_1, ..., v_6\rangle)$ ($\eta > 1$), one can enforce dealiasing.[72] For the calculations presented below, we have used an η value equal to 1.2. The presence of this pseudospectral scheme allows one to use any kind of PES expression, while some methods assume specific expression (Taylor expression for instance) of the potential. However, the use of this underlying pseudospectral scheme increases the CPU time and the memory required.

To give some information on the dimension of the working basis set and grid used to calculate highly excited states in DFCO, one can for instance consider the calculation of the state $|1,2,0,0,0,4\rangle$ whose excitation energy is about 9172 cm^{-1}. $E^{\text{tot}}_{\text{max}}$ and $E^{1,3,4,5}_{\text{max}}$ has been set to 4 eV (about 32 240 cm^{-1}) and 3 eV (about 24 180 cm^{-1}), respectively, while the following constraints on the maximum occupation was adopted: $N_1 = 7$, $N_2 = 10$, $N_3 = N_4 = 6$, $N_5 = 4$, $N_6 = 14$. It results in a working basis **B** and a grid **G** containing about 70 000 elements and 700 000 points, respectively. The validity of such drastic constraints on the maximum occupation number N_i for normal mode Q_i is checked a posteriori by analyzing the eigenstate obtained. For each eigenstate ($|\Psi\rangle = \sum_{v_1,...,v_6} c_{v_1,...,v_6} |v_1, ..., v_6\rangle$), the average quantum numbers given by $v_i^{\text{av}} = \sum_{v_1,...,v_6} v_i |c_{v_1,...,v_6}|^2$ ($i = 1, ..., 6$) are calculated to estimate the real role played by the different normal modes. For the calculated state labeled |1, 2, 0, 0, 0, 4⟩, the following average quantum numbers have been obtained: $v_1^{\text{av}} = 0.99$, $v_2^{\text{av}} = 2.1$, $v_3^{\text{av}} = 0.3$, $v_4^{\text{av}} = 0.2$, $v_5^{\text{av}} = 0.01$, $v_1^{\text{av}} = 3.6$. Large values for N_2 and N_6 are required because these two modes are strongly coupled by a Fermi resonance ($\nu_2 \simeq 2\nu_6$). This working basis set has been used to calculate all the states $|1, 4 - m, 0, 0, 0, 2m\rangle$ with $m = 0, ..., 4$, which belong to a unique polyad of states characterized by $N_{26} = 4$. Consequently, the constraints used are adapted to describe correctly these states. Specific basis set has been considered for the different polyads of states studied.

B. Determination of the Eigenstate Based on a Davidson Scheme. Wyatt is one of the theoretical chemists who showed how useful can be the Lanczos algorithm to calculate rovibrational spectrum of systems described by a large basis because this method prevents the storage of the matrix. However, the efficiency of the Lanczos algorithm decreases dramatically when the state density increases. It is the reason why we adopt for calculation of highly excited states in DFCO a diagonalization scheme based on the Davidson scheme[73] developed recently.[65,67,68] The Davidson algorithm consists of a preconditioned version of the Lanczos method. This scheme relies on the definition of a zero-order Hamiltonian $\mathbf{H}^0$, easy to use and to invert. The user gives a guess vector $|v_0\rangle$, and the Davidson scheme provides the energy E_α and the eigenstate $|\psi_\alpha\rangle$, which has the largest projection onto $|v_0\rangle$. It has been shown elsewhere[65,68,74] that the Davidson scheme is more efficient if the zero-order description of the initial guess vectors is improved. This is realized by means of a prediagonalized scheme described elsewhere[68] and briefly recalled. The overall basis set **B** is divided into two subspaces, $\mathbf{B} = \mathbf{P} \oplus \mathbf{Q}$, **P** being small enough to be directly diagonalized. Calculation of highly excited states requires a specific prediagonalization in a subspace **P**, denoted active space. **P** should contain all the zero-order states that play an active role during the calculation of the studied state or polyad of states. In this study, the active space **P** is obtained by performing a preliminary Davidson calculation in a small basis set whose dimension is limited by using some drastic but realistic energy criteria ($E^{\text{tot}}_{\text{max}}$, $E^{1,3,4,5}_{\text{max}}$) and some constraints (N_α) on the allowed v_α quantum numbers. In this first fast calculation, the guess vector $|v_0\rangle$ is the zero-order description of the studied state. This preliminary Davidson scheme gives an estimation of the studied eigenstate $|\psi^{\text{est}}_\alpha\rangle$. The zero-order states associated with the largest contributions in $|\psi^{\text{est}}_\alpha\rangle$ are retained in the **P** subspace. Then, the diagonalization of the Hamiltonian in this active space provides a new orthogonal basis set $\{|u_i\rangle, i = 1, ..., N_{\mathbf{P}}\}$ for this subspace **P** constituted by the eigenstates of the Hamiltonian. The eigenstate $|u_1\rangle$, which has the largest projection onto $|v_0\rangle$, is identified and is used as a guess vector in the following Davidson procedure performed in the large primitive basis set $\mathbf{B} = \mathbf{P} \oplus \mathbf{Q}$:

(i) Diagonalization of the Hamiltonian in the $\{u_1, ..., u_M\}$ basis set. At the beginning of the procedure, this basis contains only the guess vector u_1 obtained by the prediagonalization step. M denotes the number of Davidson iterations performed.

(ii) Selection of the Eigenstate Ψ^M with the largest projection onto u_1. This eigenstate is the best description of the exact eigenstate obtained after M iterations. The eigenvalue associated with Ψ^M is denoted E^M.

(iii) Calculation of the Residual $q = (H - E^M)\Psi^M$.

(iv) Determination of a New Vector u_{M+1}.

1. If $||\mathbf{q}|| < \epsilon$, we consider that Ψ^M is a converged eigenvector of the Hamiltonian. It has been shown elsewhere[65,68,74] that ϵ was an excellent indicator of the accuracy of the eigenvalue and the eigenvector. If ϵ is set to 10 cm^{-1}, the eigenvalue is obtained with an error smaller than 0.1 cm^{-1}, while an ϵ parameter set to 100 cm^{-1} gives the energy with an error of about 1−2 cm^{-1}. This value has been adopted to calculate highly excited states because the error generated by this Davidson scheme is smaller than the error generated by the inaccuracy of the PES used to describe the system.

2. If $||q|| > \epsilon$, a new vector u_{M+1} is generated. First, vector $\tilde{\mathbf{q}} = (E^M - H^0)^{-1}\mathbf{q}$ is calculated. Then, a new u_{M+1} orthogonalized with respect to previous vectors and normalized is calculated:

$$u_{M+1} = \frac{(1 - \sum_{m=1}^{M} |u_m\rangle\langle u_m|)\tilde{\mathbf{q}}}{||(1 - \sum_{m=1}^{M} |u_m\rangle\langle u_m|)\tilde{\mathbf{q}}||} \quad (3)$$

(v) New Davidson Iteration. The limitation of this Davidson procedure comes from the core memory required to store the M Davidson vectors u_i. This imposes some constraints on the maximum number of Davidson iterations, denoted M_{max}, performed. To preclude such core memory problem, a restart option is used. To profit from the initial Davidson scheme, N_{restart} eigenvectors Ψ^M_j ($j = 1, ..., N_{\text{restart}}$) displaying the largest projections onto the initial u_1 are kept for the next Davidson cycle. Consequently:

1. If $M + 1 < M_{\text{max}}$, a new Davidson iteration can begin: $M = M + 1$, go back to (i).

2. If $M + 1 = M_{\text{max}}$, a new Davidson cycle can begin: $M = N_{\text{restart}}$, go back to (i).

To give some practical information, the calculation of the state $|1, 2, 0, 0, 0, 4\rangle$ mentioned previously has required an active space containing about 2000 states and has been determined by performing a preliminary Davidson calculation in a small basis set containing 27 000 states. The final Davidson scheme has been applied in a basis set **B** and a grid **G** containing 70 000 states and 700 000 points, respectively. N_{max} and N_{restart} have been set to 450 and 100 in this calculation, respectively. The determination of the eigenvalue (9172 cm^{-1} of excitation energy) and the eigenstate have required two cycles of the Davidson scheme and a total of 771 iterations of the Davidson scheme.

III. Analysis of the Accuracy of the Spectrum Obtained with the Global PES

A comparison between the experimental data provided by Crane et al.[4] and the spectrum obtained by using the Davidson scheme coupled with the Jacobi−Wilson method is presented in this section. From the experimental point of view, dispersed fluorescence and stimulated emission pumping spectra of jet cooled DFCO from the $2^1 6^2$, $5^1 6^4$, $2^1 5^1 6^2$, and $5^1 6^6$ vibrational states of S_1 have been obtained. Progressions are assigned primarily to excitation in the Franck−Condon active modes ν_2, ν_5, and ν_6. Consequently, Crane et al. gave in Table 2 of ref 4 the energies and a proposition of assignment of a series of lines up to 9000 cm^{-1} of energy excitation. We focus in the present study on 48 lines of symmetry A', but a similar work can be done for the 23 lines of symmetry A''. The lines provided by experiment have been assigned by the following labels:[4]

$$\nu_i + (N_{26} - n)\nu_2 + 2n\nu_6\ (i = 1, 3, 4),\ N_{26} = 0, 1, 2, 3, 4;\ n = 0, ..., N_{26}$$

$$N_5\nu_5 + (N_{26} - n)\nu_2 + 2n\nu_6\ (N_5 = 1, 2, 3, 4),\ N_{26} = 0, 1, 2, 3, 4;\ n = 0, ..., N_{26}$$

The experimentalists considered that the spectrum is perturbed by a 266 ($\nu_2 \approx 2\nu_6$) and 233 ($\nu_2 \approx 2\nu_3$) Fermi resonances as well as a 3566 Darling−Dennisson ($\nu_3 + \nu_5 \approx 2\nu_6$). We find that the more important Fermi resonance that has to be considered is the first one that couples the out-of-plane mode

TABLE 2: Comparison between Experimental Values When They Are Available, Fitted Valued Using the 4D Model Hamitonian Developed by Experimentalists (Values Provides in Italics in This Table), Calculated Ones Using the 6D Global PES Developed by Kato and Co-workers, and Corrected Ones Taking into Account the Error Provided by the Global PES for the Energies of the Fundamental Transitions

	polyad of	$3\nu_2$	$3\nu_2+\nu_5$	$3\nu_2+\nu_3$	$3\nu_2+\nu_4$	$3\nu_2+2\nu_5$	$3\nu_2+3\nu_5$	$3\nu_2+\nu_1$
E_4	exp or *fit*[a]	*5026*	*5681*	*5992*	*6089*	*6335*	*6990*	*7234*
	calcd[b]	5045	5695	6016	6094	6343	6990	7266
	corr[c]	5021	5675	5976	6075	6325	6979	7224
	$(v_1^{av},...,v_6^{av})$[d]	(0.2, 0.5, 0.0, 0.2, 0.0, 4.8)	(0.2, 0.5, 0.2, 0.1, 1.0, 4.7)	(0.2, 0.4, 1.1, 0.1, 0.0, 4.8)	(0.2, 0.5, 0.2, 1.1, 0.1, 4.6)	(0.2, 0.5, 0.2, 0.1, 2.0, 4.6)	(0.2, 0.5, 0.2, 0.2, 3.1, 4.5)	(1.1, 0.5, 0.2, 0.1, 0.0, 4.3)
		(0.0, 0.3, 0.0, 0.0, 0.0, 5.2)	*(0.0, 0.4, 0.1, 0.0, 1.0, 5.1)*	*(0.0, 0.3, 5, 1.1, 0.0, 0.1, 4.8)*	*(0.0, 0.4, 0.0, 1.0, 0.0, 5.2)*	*(0.0, 0.4, 0.1, 0.0, 2.1., 5.1)*	*(0.0, 0.4, 0.1, 0.0, 3.1, 4.9)*	*(1.0, 0.3, 0.1, 0.0, 0.0,5.2)*
E_3	exp or *fit*[a]	5174	*5825*	*6137*	*6234*	*6475*	*7124*	*7387*
	calcd[b]	5176	5823	6147	6224	6468	7111	7408
	corr[c]	5172	5824	6132	6231	6477	7115	7389
	$(v_1^{av},...,v_6^{av})$[d]	(0.1, 1.2, 0.1, 0.1, 0.0, 3.4)	(0.2, 1.2, 0.1, 0.1, 1.1, 3.2)	(0.2, 1.2, 1.1, 0.2, 0.1, 3.3)	(0.2, 1.2, 0.2, 1.2, 0.2, 3.0)	(0.2, 1.2, 0.2, 0.2, 2.1, 3.0)	(0.2, 1.2, 0.2, 0.4, 3.4, 2.6)	(1.0, 1.2, 0.2, 0.1, 0.0, 3.5)
		(0.0, 1.1, 0.0, 0.0, 0.0, 3.7)	*(0.0, 1.1, 0.0, 0.0, 1.0, 3.7)*	*(0.0, 1.1, 1.1, 0.0, 0.0, 3.6)*	*(0.0, 1.1, 0.0, 1.0, 0.0, 3.7)*	*(0.0, 1.1, 0.1, 0.0, 2.0, 3.6)*	*(0.0, 1.2, 0.1, 0.0, 3.1, 3.4)*	*(1.0, 1.1, 0.0, 0.0, 0.0, 3.8)*
E_2	exp or *fit*[a]	5288	*5934*	6250	*6344*	6581	7228	7505
	calcd[b]	5267	5910	6240	6314	6552	7194	7508
	corr[c]	5291	5940	6251	6347	6588	7234	7516
	$(v_1^{av},...,v_6^{av})$[d]	(0.1, 2.1, 0.1, 0.1, 0.0, 1.6)	(0.1, 2.1, 0.1, 0.1, 1.0, 1.5)	(0.1, 2.1, 1.1, 0.2, 0.0, 1.6)	(0.1, 2.1, 0.1, 1.2, 0.0, 1.3)	(0.1, 2.1, 0.1, 0.1, 2.0, 1.4)	(0.1, 2.0, 0.1, 0.1, 3.0, 1.3)	(0.9, 2.0, 0.3, 0.2, 0.2, 1.7)
		(0.0, 2.0, 0.2, 0.0, 0.0, 2.0)	*(0.0, 2.0, 0.0, 0.0, 1.0, 2.0)*	*(0.0, 2.0, 1.1, 0.0, 0.0, 2.0)*	*(0.0, 2.0, 0.1, 1.0, 0.0, 2.0)*	*(0.0, 2.0, 0.0, 0.0, 2.0, 1.9)*	*(0.0, 2.0, 0.0, 0.0, 3.0, 1.8)*	*(1.0, 1.9, 0.1, 0.0, 0.0, 2.1)*
E_1	exp or *fit*[a]	5348	5993	6309	*6401*	6638	7283	7571
	calcd[b]	5320	5963	6293	6371	6606	7249	7564
	corr[c]	5343	5988	6303	6394	6632	7276	7575
	$(v_1^{av},...,v_6^{av})$[d]	(0.1, 2.1, 0.1, 0.1, 0.0, 1.7)	(0.1, 2.0, 0.1, 0.1, 1.0, 1.9)	(0.1, 2.0, 1.0, 0.2, 0.0, 1.7)	(0.1, 1.9, 0.1, 1.1, 0.0, 2.0)	(0.1, 1.9, 0.1, 0.1, 2.0, 2.1)	(0.1, 1.8, 0.1, 0.1, 3.0, 2.2)	(0.9, 2.1, 0.1, 0.2, 0.0, 1.7)
		(0.0, 2.5, 0.0, 0.0, 0.0, 0.9)	*(0.0, 2.5, 0.0, 0.0, 1.0, 1.0)*	*(0.0, 2.5, 1.1, 0.0, 0.0, 0.9)*	*(0.0, 2.4, 0.0, 1.0, 0.0, 1.0)*	*(0.0, 2.4, 0.0, 0.0, 2.0, 1.2)*	*(0.0, 2.3, 0.0, 0.0, 3.0, 1.3)*	*(1.0, 2.6, 0.0, 0.0, 0.0, 0.7)*

[a] When experimental values are not available, the values provided by the very simple experimentalist modelization developed in ref 4 and summarized in Section III (near eq 4) are given. [b] Calculated values using the global PES.[72] [c] Corrected values using eq 5. [d] Average quantum number obtained either with the global PES and the Davidson scheme or in italics with the 4D model Hamiltonian developed by Moore and co-workers.[4]

ν_6 with the CO stretch ν_2. Consequently, a study of polyads of coupled states has been performed: a polyad can be characterized by the quantum number N_{26}. The 48 energies observed by the experiment belong to 30 different polyads of states. We have calculated all the energies and the eigenstates that belong to these 30 polyads of states: 84 eigenstates have been calculated. The calculation of all these states will be used in Section IV to analyze the structure of the spectrum and the efficiency of the different resonances.

In the sophisticated and detailed experimental study performed by Crane et al.,[4] a fit of the experimental data has been proposed. First, they tried to fit the spectrum by using a standard Dunham-type expression:

$$E(v_1, ..., v_6) = \sum_{i=1}^{6} \omega_i v_i + \sum_{i=1}^{6}\sum_{j=i}^{6} x_{ij} v_i v_j \qquad (4)$$

This basic approach was not sufficient to fit all the experimental data up to 9000 cm^{-1}. Consequently, they have included in the fit three coupling constants: k_{266}, k_{233}, and k_{3566}. This very simple model Hamiltonian was diagonalized for each polyad of states coupled by these three constants. The determination of these 3 force constants k_{266}, k_{233}, and k_{3566}, the six ω_i ($i = 1, ..., 6$) and the 19 x_{ij} constants was based on the use of a simulated annealing optimization routine.[4] Figure 2 represents the error between the fitted and the experimental spectrum (circles in Figure 2): the agreement is excellent. In Table 2 and Figure 4 of Section IV, we compare the eigenstates obtained either by this modelization (values provided in italics in Table 2 and Figure 4) or by a 6D variational calculation. We can now discuss the accuracy of the spectrum provided by the global six-dimensional PES developed by Kato and co-workers.[75] This PES includes the dissociation pathway and was constructed with the use of about 4000 ab initio potential energies computed at the (RHF)/MP2 level. The aim of such a sophisticated PES is to describe highly excited states of HFCO or DFCO molecules. This PES has not been fitted to reproduce the spectrum. It is the reason why it is crucial to compare the experimental and calculated data to quantify the quality of this global PES. Squares in Figure 2 reproduce the difference between the numerical spectrum obtained with this PES and the experimental data. One can mention that the error is mainly generated by the inaccuracy of the PES because the error caused by the Davidson scheme and the finite dimension of the working basis set is significantly smaller (few cm^{-1}) for highly excited states. What is the major origin of the difference between experimental and calculated spectra? Table 1 provides the error generated by the PES for the fundamental transitions for the A' modes and for the first overtone for the A'' out-of-plane mode. What is the consequence of this error (reproduced in column 4 of Table 1) on the calculation of highly excited states? To answer to this question, a corrected value of the energy associated to a given eigenstate ($|\Psi\rangle = \sum_{v_1,...,v_6} c_{v_1,...,v_6} |v_1, ..., v_6\rangle$) has been estimated:

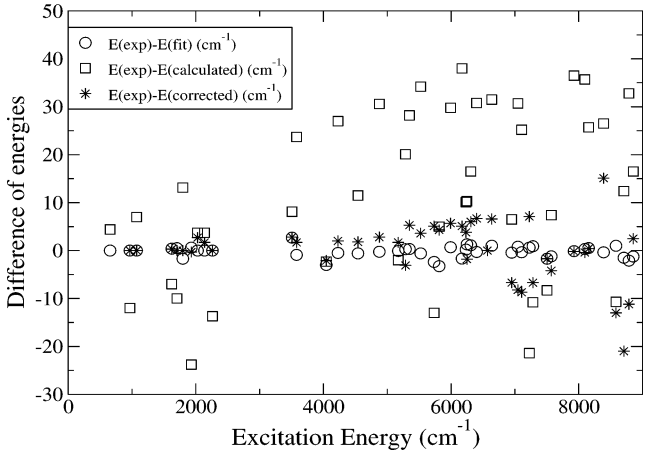

Figure 2. Difference between experimental data with the fitted one by Crane et al. (circles) or using the variational calculation using the Kato's PES (squares) or the corrected energy according to eq 5. All the energies are expressed in cm^{-1}.

(1) First, the average quantum number in mode Q_i given by $v_i^{av} = \sum_{v_1,...,v_6} v_i |c_{v_1,...,v_6}|^2$ is calculated to estimate the real role played by the different normal modes Q_i in $|\Psi\rangle$.

(2) Second, the corrected value of the energy is given by:

$$E^{corr} = E^{calcd} + \sum_{i=1}^{6} \Delta\nu_i v_i^{av} \qquad (5)$$

The $\Delta\nu_i$ ($i = 1$, ..., 6) are fitted to obtain $E^{corr} = E^{exp}$ for the A' fundamental transitions and for the first out-of-plane overtone. The values of $\Delta\nu_i$ ($i = 1$, ..., 6) are provided in column 5 of Table 1. Columns 4 and 5 are different because of the existence of Fermi resonances, which efficiently couple modes even for these low excited states.

Stars in Figure 2 provides the corrected values of the energies up to 9000 cm^{-1}. This figure shows that there is a satisfactory agreement between the experimental data and the corrected ones. This very simple approach allows to improve the energies provided by the variational calculation and requires only the knowledge of the fundamental A' transition and the first out-of-plane overtone. Consequently, this approach is predictive. This section establishes that the PES developed by Kato and co-workers gives a very good description of the intermode couplings in this molecule even for highly excited-state while the spectrum is strongly perturbed by resonances. The error on highly excited states can be significantly reduced by taking into account the error generated on the calculation of the fundamental A' transitions and the first out-of-plane overtone.

IV. Analysis of the Structure of the Spectrum Generated by an Efficient Fermi Resonance

This section is dedicated to the analysis of the structure of DFCO spectrum and the determination of the role played by the different resonances. In fact, one of the aims of the experimental study was to compare the dynamical behaviors of HFCO and DFCO. HFCO is an excellent prototype to study mode specificity in unimolecular dissociation because the out-of-plane mode (ν_6) is weakly coupled to the reaction coordinate that lies entirely in the molecular plane. HFCO has been the subject of intensive experimental studies conducted by Moore and co-workers[3,76,77] and numerical simulations.[32,74,75,78,79] The aim of these studies was to analyze the energy flow through a HFCO molecule whose out-of-plane was highly excited. Then, Moore and co-workers[4,5] focus on DFCO because of the existence of resonances that might couple the out-of-plane mode with in-plane modes. The experiments seem to predict that the IVR dynamics in DFCO is very different from the very strong mode-specific IVR dynamic in HFCO. In particular, the quasistability of large amplitude out-of-plane vibrations in HFCO is destroyed in DFCO, probably due to a 266 resonance, which is not efficient in HFCO. Our group has investigated the IVR in DFCO[33] whose out-of-plane is highly excited by using the MCTDH code[24−26] to propagate the initial wave packet. In agreement with the experimental findings, our study proves that the IVR dynamics of DFCO are in marked contrast to the dynamic of HFCO. Above all, the IVR in DFCO is affected by the presence of the 266 resonance. This resonance seems to be the main reason that explains why the experimental spectra is perturbed and more "congested" above the dissociation. However, the theoretical study shows that the CO stretch itself (mode 2) is not coupled to the other in-plane modes. Consequently, the system remains mode specific. The present analysis of the spectrum up to 9000 cm^{-1} will help to understand the very original dynamical behavior of DFCO. First, the role played by the modes 1, 3, 4, and 5 has been quantified: for the 84 bands calculated, the average quantum numbers v_i^{av} ($i = 1$, 3, 4, 5) have been calculated and represented in Figure 3. It is remarkable to note that the average quantum number v_i^{av} is very similar to the integer quantum number v_i proposed in the label, i.e., $v_i^{av} \simeq 0$ *or* 1for $i = 1$, 3, 4 and $v_5^{av} \simeq 0$, 1, 2, 3, 4. That establishes that there is no efficient coupling between these modes and modes 2 and 6. It shows that modes 2 and 6 are really decoupled to these modes. The experimental study[4,5] predicts that 233 and 3566 resonances should be also efficient. In fact, the effect of these resonances is not significative. For instance, the v_3^{av} is very small (less than 0.3) in the $m\nu_2$ overtones ($m = 1$, ..., 5). Figure 4 represents the general structure of a polyad of states characterized by $N_{26} = 1$, 2, 3, 4. We have reproduced in Figure 4 the values obtained for the corrected energies and for the couple of average quantum numbers (v_2^{av}, v_6^{av}) for the polyads of states that are generated by the mixing of the following ($N_{26} + 1$) zero-order states: $\{|(N_{26} - n)\nu_2 + 2n\nu_6\rangle^0; n = 0, ..., N_{26}\}$. The values written in italics are provided by the 4D very simple modelization developed by experimentalists. First, in agreement with experimental predictions, an increase of the coupling between modes 2 and 6 is observed when the excitation energy increases. While the weight of mode 6 is larger in the low-energy bands of a given polyad, an intense mixing of modes 2 and 6 is predicted in the energy levels (E_1, E_2) for $N_{26} = 3$ and energy levels (E_1, E_3) for $N_{26} = 4$. It is very interesting to be able to label these bands by the average

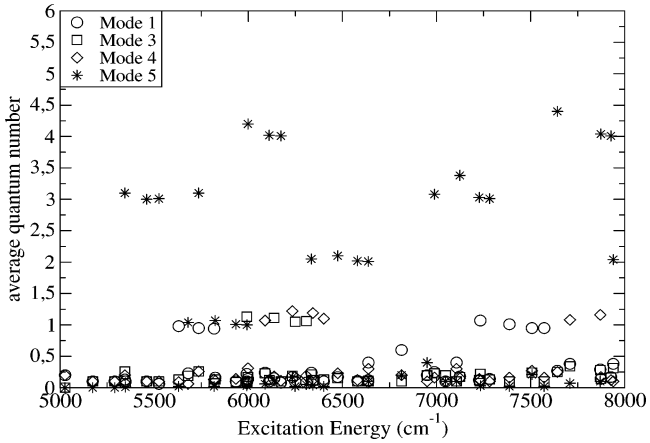

Figure 3. Average quantum number for modes 1, 3, 4, and 5 for all the calculated states.

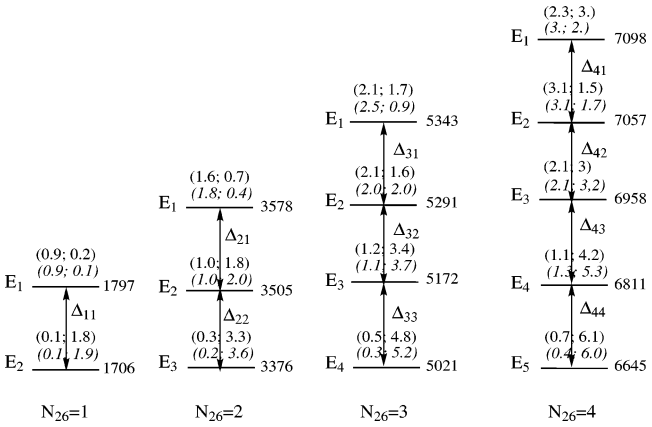

Figure 4. Splitting obtained for the polyads generated by the coupling of the states $\{ |(N_{26} - n)\nu_2 + 2n\nu_6\rangle^o, n = 0, ..., N_{26}\}$ with $N_{26} = 1, 2, 3, 4$. For each corrected energy (expressed in cm^{-1}), the average quantum numbers (v_2^{av}, v_6^{av}) are provided. The values written in italics are obtained with the 4D modelization developed by the experimentalists, while the other values are provided by the 6D variational calculation.

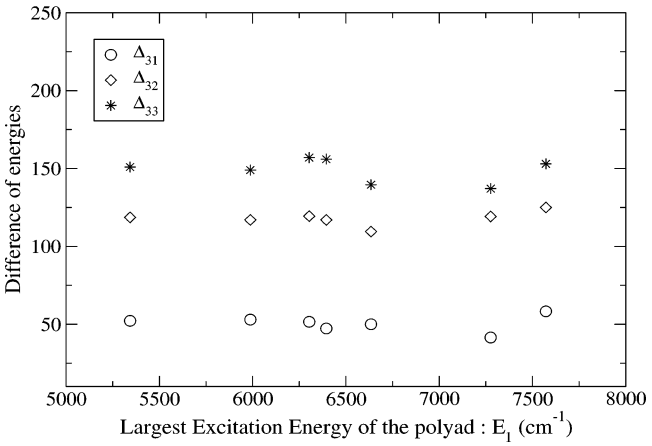

Figure 5. Splitting for $N_{26} = 3$ for different polyads generated by the coupling of $\{|(v_i + N_{26} - n)\nu_2 + 2n\nu_6\rangle^o, n = 0, ..., N_{26}\}$ with $i = 1, 3, 4$ or $\{N_5\nu_5 + |(N_{26} - n)\nu_2 + 2n\nu_6\rangle^o, n = 0, ..., N_{26}\}$ with $N_5 = 1, 2, 3$.

quantum number because it is totally impossible to identify theses bands by a unique zero-order state. We can now compare the values provided by the variational calculations and the 4D model proposed by experimentalists. The very original evolution of v_i^{av} ($i = 2, 6$) in a given polyad is not exactly reproduced by the 4D model, which totally neglects mode 1 and 4. The 6D variational calculation shows the role played by the in-plane modes: small but not totally negligible. They are responsible of the evolution of the v_i^{av} ($i = 2, 6$) in a given polyad. We focus now on the polyads generated by the mixing of states such that $\{|v_i + (N_{26} - n)\nu_2 + 2n\nu_6\rangle^0, n = 0, ..., N_{26}\}$ for $N_{26} = 3$ and $i = 1, 3, 4$ or $\{|N_5\nu_5 + (N_{26} - n)\nu_2 + 2n\nu_6\rangle^0, n = 0, ..., N_{26}\}$ for $N_5 = 1, 2, 3$ and $N_{26} = 3$. How modified is the structure of the spectrum of these polyads of states by the fact that an in-plane mode 1 or 3 or 4 or 5 is excited? Figure 5 provides the splittings (Δ_{31}, Δ_{32}, Δ_{33} defined in Figure 4) calculated for the polyads of states characterized by $N_{26} = 3$. This figure shows that the splittings are not significantly affected by the excitation of modes 1, 3, 4, 5. The average quantum numbers in modes 2 and 6 are reproduced in Figures 6 and 7 for these bands. Table 2 gives the energies (experimental ones, variational ones and corrected ones) and the average quantum numbers (v_1^{av}, ..., v_6^{av}) obtained either by the 6D variational calculation or by the 4D modelization proposed by Moore and co-workers. It is remarkable to note how these quantities are not affected by the excitation of the modes 1, 3, 4, 5 even when mode 5 is excited by 3 quanta. Figures 5−7 and Table 2 focus on the $N_{26} = 3$ polyad, but similar trends are observed for the other polyads ($N_{26} = 1, 2, 3, 4$). This analysis demonstrates how the coupling scheme between modes 2 and 6 is independant of the excitation of the other modes. Its explains why the IVR predicted in DFCO is mode selective: the energy initially deposited in mode 6 is transferred in a reversible way in modes 2 and 6. However, the transfer to mode 1, 3, 4, and 5 is slow because the couplings are not efficient.

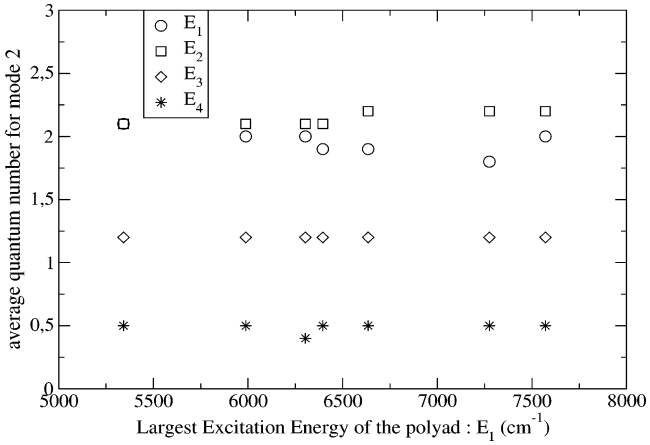

Figure 6. Average quantum number for mode 2 for polyads caracterized by $N_{26} = 3$.

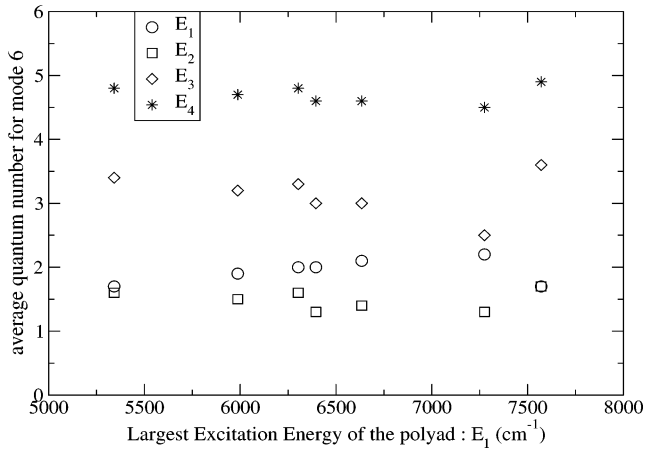

Figure 7. Average quantum number for mode 6 for polyads caracterized by $N_{26} = 3$.

V. Conclusions

First, this study has shown that the Davidson scheme coupled to the JW parametrization and a specific prediagonalization step is able to provide highly excited states even when strong and efficient Fermi resonances exist. Up to now, this method has been used either in HFCO where the intermode couplings are small or in H_2CO where the state density is smaller. Second, the comparison between the experimental and calculated spectra has established the great quality of the global PES developed by Kato and co-workers. We show also that the energies provided by this PES can be easily corrected by taking into account the error observed for the fundamental frequencies. The PES, used in a recent dynamical study,[33] reproduces correctly the intermode couplings in DFCO. Third, the analysis of the eigenstates up to 9000 cm^{-1} of excitation has demonstrated that the modes 2 and 6 are decoupled to the other modes, while the

experimental studies suggest that some other resonances might be efficient to couple mode 2 with mode 3, for instance. In fact, such a Fermi resonance is not efficient up to 9000 cm^{-1}. This analysis helps to understand the IVR study performed recently.[32] Finally, we are planning to implement the dipole momenta as well as the overall rotation of the molecule to carry out simulations in the presence of a time-dependent field. We will compare the dynamical behavior of HFCO and DFCO excited by a laser pulse and will estimate the influence of this Fermi resonance to the dynamical behavior of DFCO.

Acknowledgment. Professor Claude Leforestier is warmly thanked for his crucial role in the development of the code used in this study. Fabien Gatti is also warmly thanked for fruitful discussion and comments on this study.

References and Notes

(1) A. H. Zewail. *Femtochemistry: Ultrafast Dynamics of the Chemical Bond*; World Scientific: Singapore, 1994.
(2) Nesbitt, D.; Field, R. *J. Phys. Chem.* **1996**, *100*, 12735.
(3) Choi, Y. S.; Moore, C. B. *J. Chem. Phys.* **1991**, *94*, 5414−5425.
(4) Crane, J. C.; Kawai, A.; Nam, H.; Clauberg, H.; Beal, H. P.; Guinn, P.; Moore, C. B. *J. Mol. Spectrosc.* **1997**, *183*, 273−284.
(5) Crane, J. C.; Nam, H.; Clauberg, H.; Beal, H. P.; Kalinovski, I. J.; Shu, R. G.; Moore, C. B. *J. Phys. Chem. A* **1998**, *102*, 9433.
(6) Campargue, A.; Stoeckel, F. *J. Chem. Phys.* **1986**, *85*, 1220−1227.
(7) Romanini, D.; Campargue, A. *Chem. Phys. Lett.* **1996**, *254*, 52.
(8) Boyarkin, O.; Rizzo, T.; Perry, D. *J. Chem. Phys.* **1999**, *110*, 11346.
(9) Boyarkin, O.; Rizzo, T. *J. Chem. Phys.* **1995**, *103*, 1985.
(10) Boyarkin, O.; Rizzo, T. *J. Chem. Phys.* **1996**, *105*, 6285.
(11) McDonald, P. A.; Shirk, J. S. *J. Chem. Phys.* **1982**, *77*, 2355.
(12) Khriatchev, L.; Lundell, J.; Isoniemi, E.; Räsänen, M. R. *J. Chem. Phys.* **2000**, *113*, 4265−4273.
(13) Page, R.; Shen, Y.; Lee, Y. *J. Chem. Phys.* **1988**, *88*, 4621.
(14) Callegari, A.; Merker, U.; Engels, P.; Srivastava, H.; Lehmann, K.; Scoles, G. *J. Chem. Phys.* **2000**, *113*, 10583.
(15) Lehman, K. K.; Scoles, G.; Pate, B. H. *Annu. Rev. Phys. Chem.* **1994**, *45*, 241.
(16) Iung, C.; Ribeiro, F.; Sibert, E. L. *J. Phys. Chem. A* **2006**, *110*, 5420.
(17) Burleigh, D. C.; McCoy, A. B.; E. L. S., III. *J. Chem. Phys.* **1996**, *104*, 480.
(18) Wang, X.-G.; Sibert, E. L.; Martin, J. *J. Chem. Phys.* **2000**, *112*, 1353.
(19) Castillo-Chará, J.; Sibert, E. L. *J. Chem. Phys.* **2004**, *119*, 11671.
(20) Ramesh, S. G.; Sibert, E. L. *Mol. Phys.* **2005**, *103*, 149.
(21) Ramesh, S. G.; Sibert, E. L. *J. Chem. Phys.* **2004**, *120*, 11011.
(22) Neuhauser, D. *J. Chem. Phys.* **1990**, *93*, 2611.
(23) Wall, M. R.; Neuhauser, D. *J. Chem. Phys.* **1995**, *102*, 8011.
(24) Worth, G. A.; Beck, M. H.; Jäckle, A.; Meyer, H.-D. *The MCTDH Package*, version 8.2, 2000; H.-D. version 8.3, 2002. See http://www.pci-.uniheidelberg. de/tc/usr/mctdh/.
(25) Meyer, H.-D.; Manthe, U.; Cederbaum, L. S. *Chem. Phys. Lett.* **1990**, *165*, 73−78.
(26) Manthe, H.-D.; Meyer, U.; Cederbaum, L. S. *J. Chem. Phys.* **1992**, *97*, 3199−3213.
(27) Gatti, F.; Meyer, H.-D. *Chem. Phys.* **2004**, *304*, 3−15.
(28) Beck, M. H.; Meyer, H.-D. *J. Chem. Phys.* **1998**, *109*, 3730−3741.
(29) Richter, F.; Hochlaf, M.; Rosmus, P.; Gatti, F.; Meyer, H.-D. *J. Chem. Phys.* **2004**, *120*, 1306−1317.
(30) Richter, F.; Rosmus, P.; Gatti, F.; Meyer, H.-D. *J. Chem. Phys.* **2004**, *120*, 6072−6084.
(31) Iung, C.; Gatti, F.; Meyer, H.-D. *J. Chem. Phys.* **2004**, *120*, 6992−6998.
(32) Pasin, G.; Gatti, F.; Iung, C.; Meyer, H.-D. *J. Chem. Phys.* **2006**, *124*, 194304.
(33) Pasin, G.; Gatti, F.; Iung, C.; Meyer, H.-D. *J. Chem. Phys.* **2007**, *126*, 024302.
(34) Meyer, H.-D.; Quéré, F. L.; Léonard, C.; Gatti, F. *Chem. Phys.* **2006**, *329*, 179−192.
(35) Richter, F.; Léonard, C.; Quéré, F. L.; Gatti, F.; Meyer, H.-D. *J. Chem. Phys.* in press.
(36) Pasin, G.; Léonard, C.; Quéré, F. L.; Gatti, F.; Iung, C.; Meyer, H.-D. 2007, to be published.
(37) Sibert, E. L. *J. Chem. Phys.* **1988**, *88*, 4378.
(38) Carbonnière, P.; Begue, D.; Pouchan, C. *Chem. Phys. Lett.* **2004**, *393*, 92.
(39) Begue, D.; Carbonnière, P.; Barone, V.; Pouchan, C. *Chem. Phys. Lett.* **2005**, *415*, 25.
(40) Begue, D.; Carbonnière, P.; Barone, V.; Pouchan, C. *Chem. Phys. Lett.* **2005**, *416*, 206.
(41) Wyatt, R. E., Zhang, J. Z. H., Eds. *Dynamics of Molecules and Chemical Reactions*; Marcel Dekker: New York, 1996.
(42) Nauts, A.; Wyatt, R. E. *Phys. Rev. Lett.* **1983**, *51*, 2238.
(43) Wyatt, R. E. *Adv. Chem. Phys.* **1989**, *53*, 231.
(44) Lanczos, C. *J. Res. Natl. Bur. Stand.* **1950**, *45*, 255.
(45) Iung, C.; Leforestier, C.; Wyatt, R. E. *J. Chem. Phys.* **1993**, *98*, 6722.
(46) Iung, C.; Wyatt, R. E. *J. Chem. Phys.* **1993**, *99*, 2261−2264.
(47) Bloch, C. *Nucl. Phys.* **1958**, *6*, 329.
(48) Maynard, A.; Wyatt, R. E.; Iung, C. *J. Chem. Phys.* **1997**, *106*, 9483.
(49) Maynard, A.; Wyatt, R. E.; Iung, C. *J. Chem. Phys.* **1995**, *103*, 8372.
(50) Wyatt, R. E.; Iung, C.; Leforestier, C. *Acc. Chem. Res.* **1995**, *28*, 423.
(51) Ericsson, T.; Ruhe, A. *Math. Comput. Res.* **1980**, *35*, 1251.
(52) Wyatt, R. *Phys. Rev. E* **1995**, *51*, 3643.
(53) Minehard, T.; Adcock, J.; Wyatt, R. *Phys. Rev. E* **1997**, *56*, 4837.
(54) Vijay, A.; Wyatt, R. E. *Phys. Rev. E* **2000**, *62*, 4351.
(55) Wang, S.; Carrington, J. *J. Chem. Phys.* **2000**, *112*, 8765.
(56) Poirier, B.; Carrington, T., Jr. *J. Chem. Phys.* **2001**, *114*, 9254.
(57) Poirier, B.; Carrington, T., Jr. *J. Chem. Phys.* **2002**, *116*, 1215.
(58) Bian, W.; Poirier, B. *J. Theor. Comput. Chem.* **2003**, *2*, 583.
(59) Bian, W.; Poirier, B. *J. Chem. Phys.* **2004**, *121*, 4467.
(60) Poirier, B.; Light, J. *J. Chem. Phys.* **2003**, *118*, 3458.
(61) Poirier, B.; Miller, W. *Chem. Phys. Lett.* **1997**, *265*, 77.
(62) Wyatt, R. E.; Iung, C.; Leforestier, C. *J. Chem. Phys.* **1992**, *97*, 3458.
(63) Wyatt, R. E.; Iung, C.; Leforestier, C. *J. Chem. Phys.* **1992**, *97*, 3477.
(64) Wyatt, R. E.; Iung, C. *J. Chem. Phys.* **1993**, *98*, 6758.
(65) Ribeiro, F.; Iung, C.; Leforestier, C. *J. Chem. Phys.* **2005**, *123*, 054106.
(66) Leforestier, C.; Viel, A.; Gatti, F.; Munoz, C.; Iung, C. *J. Chem. Phys.* **2001**, *114*, 2099.
(67) Ribeiro, F.; Iung, C.; Leforestier, C. *Chem. Phys. Lett.* **2002**, *362*, 199.
(68) Ribeiro, F.; Iung, C.; Leforestier, C. *J. Theor. Comput. Chem.* **2003**, *2*, 609.
(69) Iung, C.; Gatti, F. *Int. J. Quantum Chem.* **2006**, *106*, 130.
(70) Gatti, F.; Iung, C. *J. Theor. Comput. Chem.* **2003**, *2*, 507−522.
(71) Wilson, E.; Decius, J. and P. *Cross Molecular Vibrations*; McGraw-Hill: New York, 1955.
(72) Friesner, R. A. *J. Chem. Phys.* **1985**, *85*, 1462.
(73) Davidson, E. *J. Comput. Phys.* **1975**, *17*, 87.
(74) Iung, C.; Ribeiro, F. *J. Chem. Phys.* **2005**, *121*, 174105.
(75) Yamamoto, T.; Kato, S. *J. Chem. Phys.* **1997**, *107*, 6114−6122.
(76) Choi, Y. S.; Moore, C. B. *J. Chem. Phys.* **1992**, *97*, 1010−1021.
(77) Choi, Y. S.; Moore, C. B. *J. Chem. Phys.* **1995**, *103*, 9981−9988.
(78) Yamamoto, T.; Kato, S. *J. Chem. Phys.* **2000**, *112*, 8006−8016.
(79) Yamamoto, T.; Kato, S. *J. Chem. Phys.* **1998**, *109*, 9783−9793.